

Mechanism and Origins of Selectivity in Ru(II)-Catalyzed Intramolecular (5+2) Cycloadditions and Ene Reactions of Vinylcyclopropanes and Alkynes from Density Functional Theory

Xin Hong,[†] Barry M. Trost,^{*,‡} and K. N. Houk^{*,†}

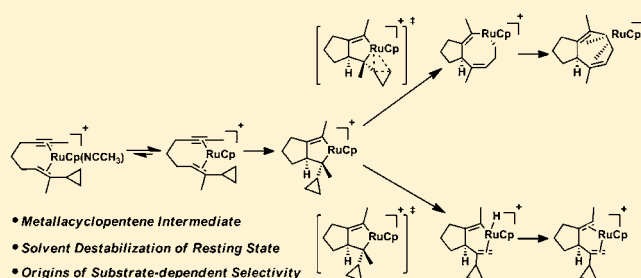
[†]Department of Chemistry and Biochemistry, University of California, Los Angeles, California 90095-1569, United States

[‡]Department of Chemistry, Stanford University, Stanford, California 94305-5080, United States

Supporting Information

ABSTRACT: The mechanism, solvent effects, and origins of selectivities in Ru(II)-catalyzed intramolecular (5+2) cycloaddition and ene reaction of vinylcyclopropanes (VCPs) and alkynes have been studied using density functional theory. B3LYP/6-31G(d)/LANL2DZ optimized structures were further evaluated with the M06 functional, 6-311+G(2d,p) and LANL2DZ basis sets, and the SMD solvent model. The favored mechanism involves an initial ene-yne oxidative cyclization to form a ruthenacyclopentene intermediate. This mechanism is different from that found earlier with rhodium

catalysts. The subsequent β -hydride elimination and cyclopropane cleavage are competitive, determining the experimental selectivity. In *trans*-VCP, the cyclopropane cleavage is intrinsically favored and leads to the (5+2) cycloaddition product. Although the same intrinsic preferences occur with the *cis*-VCP, an unfavorable rotation is required in order to generate the *cis*-double bond in seven-membered ring product, which reverses the selectivity. Acetone solvent is found to facilitate the acetonitrile dissociation from the precatalyst, destabilizing the resting state of the catalyst and leading to a lower overall reaction barrier. In addition, the origins of diastereoselectivities when the allylic hydroxyl group is *trans* to the bridgehead hydrogen are found to be the electrostatic interactions. In the pathway that generates the favored diastereomer, the oxygen lone pairs from the substituent are closer to the cationic catalyst center and provide stabilizing electrostatic interactions. Similar pathways also determine the regioselectivities, that is, whether the more or less substituted C–C bond of cyclopropane is cleaved. In the *trans*-1,2-disubstituted cyclopropane substrate, the substituent from the cyclopropane is away from the reaction center in both pathways, and low regioselectivity is found. In contrast, the cleavage of the more substituted C–C bond of the *cis*-1,2-disubstituted cyclopropane has steric repulsions from the substituent, and thus higher regioselectivity is found.



INTRODUCTION

Seven-membered carbocycles are present in many natural products and drugs and have been targets for a number of synthetic studies (Scheme 1).¹ The synthesis of seven-membered rings often requires ring-closing bond formation or ring expansion reactions.² These transformations typically need multistep synthesis of precursor, and thus it is difficult to achieve atom and step economy as well as application in total synthesis of fused ring systems.

Although the synthesis of seven-membered ring still lags behind that for smaller rings (especially for catalytic and intermolecular reactions), remarkable progress has been made.³ As a homologue of the Diels–Alder (4+2) cycloaddition, transition-metal-catalyzed (5+2) cycloaddition of vinylcyclopropanes (VCPs) and 2π components provides a practical and efficient way for functionalized seven-membered ring formation (Scheme 2).⁴ In 1995, the Wender group reported the first examples of intramolecular (5+2) cycloaddition of VCPs catalyzed by $[\text{Rh}(\text{Cl})(\text{PPh}_3)_3]$ and successfully applied this methodology with various catalysts, VCPs, and substrates.⁵ The

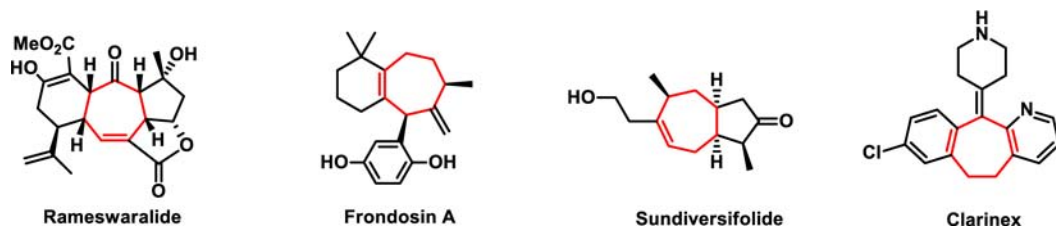
(5+2) cycloaddition has also provided a conceptual foundation and led to the application in total synthesis⁶ and the discovery of many new cycloaddition reactions, such as (5+2+1),⁷ (5+1+2+1),⁸ (3+2),⁹ and (5+1)¹⁰ reactions.

There are two general mechanisms proposed for the transition-metal-catalyzed (5+2) cycloaddition (Scheme 3). One involves the formation of a metallacyclohexene intermediate followed by 2π insertion and reductive elimination. The other proceeds through oxidative cyclization followed by cyclopropane cleavage and reductive elimination. Our previous theoretical studies have revealed that the metallacyclohexene pathway is preferred with rhodium catalysts and the rate-determining step is the 2π insertion to form the metallacyclooctadiene intermediate.¹¹ Later experimental and theoretical collaborations demonstrated a delicate electronic and steric control of regioselectivities in Rh(I)-catalyzed (5+2) cycloadditions.¹²

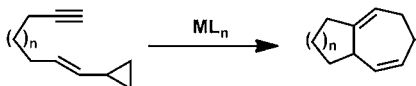
Received: February 4, 2013

Published: April 9, 2013

Scheme 1. Representative Natural Products and Drug Molecules That Contain Seven-Membered Rings



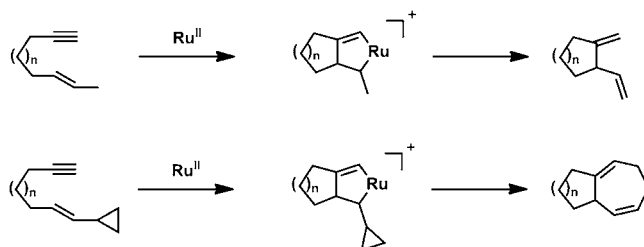
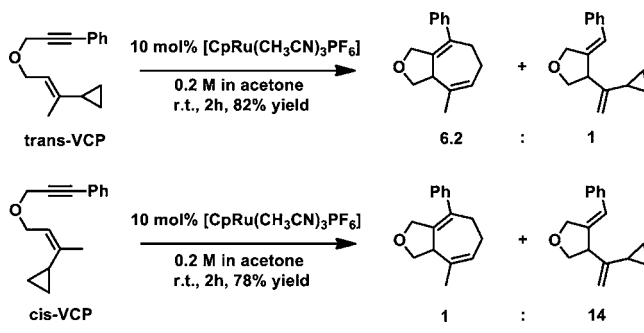
Scheme 2. General Transition-Metal-Catalyzed Intramolecular (5+2) Cycloaddition of Vinylcyclopropane and Alkyne



Inspired by the Rh(I)-catalyzed (5+2) cycloaddition and Ru(II)-catalyzed Alder ene reaction,¹³ Trost proposed a Ru(II)-catalyzed (5+2) cycloaddition involving a ruthenacyclopentene intermediate (Scheme 4).¹⁴ By replacing the terminal methyl group of the alkene with cyclopropane, a ruthenacyclopentene intermediate could be generated, leading to a seven-membered ring product by ring expansion. This chemical transformation was indeed achieved by using the $[CpRu(CH_3CN)_3PF_6]$ catalyst, the same complex that catalyzes the alkene-alkyne coupling.¹⁵ Later, Trost et al. systematically studied the scope of this reaction, including the functional group tolerance, the type and length of the tether between alkyne and VCP, and the substituent effects on the regio- and diastereoselectivities.^{14d}

The preliminary experimental studies of the mechanism pointed to the metallacyclopentene intermediate, and the discovery of the β -hydride elimination side product also supported the hypothesis of the ruthenacyclopentene intermediate (Scheme 5).^{14d} The β -hydride elimination product is quite common in Ru(II)-catalyzed (5+2) cycloaddition if the internal alkene carbon of VCP contains a substituent with an α -hydrogen and the selectivity between the (5+2) cycloaddition and ene reaction relies heavily on the substrates. The *trans*-VCP favors the (5+2) cycloaddition, and the *cis*-VCP favors the ene reaction (Scheme 5). Although the metallacyclopentene intermediate is achievable with ruthenium catalysts, the same ruthenium catalyst is also known to catalyze the vinylcyclopropane cleavage under similar conditions.¹⁶ Therefore, the ruthenacyclohexene intermediate might still compete with the ruthenacyclopentene intermediate. To understand the

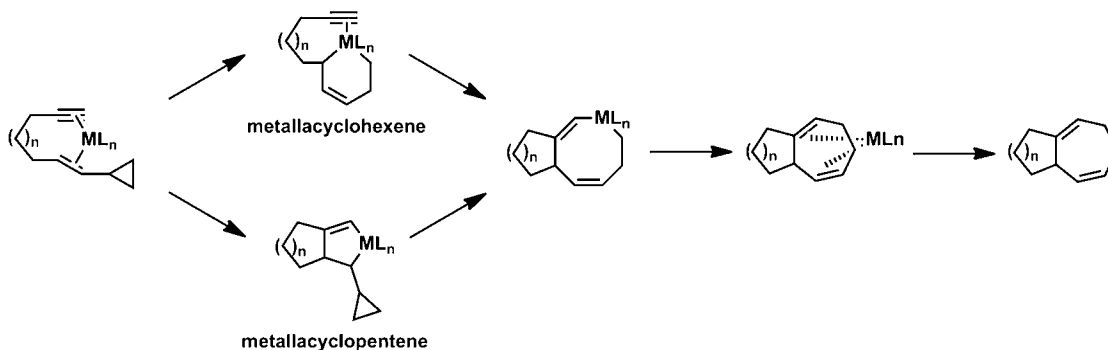
Scheme 4. Ru(II)-Catalyzed Alder Ene Reaction and (5+2) Cycloaddition

Scheme 5. Selectivity between Ru(II)-Catalyzed Intramolecular (5+2) Cycloaddition and Ene Reaction of *trans*- and *cis*-VCP

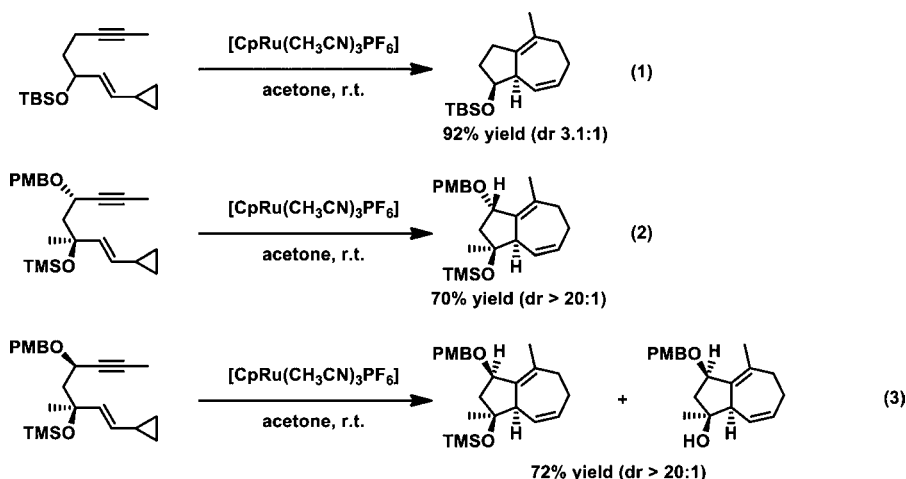
detailed mechanism of Ru(II)-catalyzed (5+2) cycloaddition was a principal goal of this work.

In addition to the questions of mechanism, a distinct solvent effect was found experimentally: the reaction requires a polar solvent, and acetone was found especially effective.^{14d} Does acetone just provide a polar solvent environment that facilitates the catalytic transformation, or is the acetone acting as a ligand? Is acetone stabilizing the rate-determining transition state or destabilizing the resting state to lower the overall reaction barrier? Although solvent effect is very crucial and common in

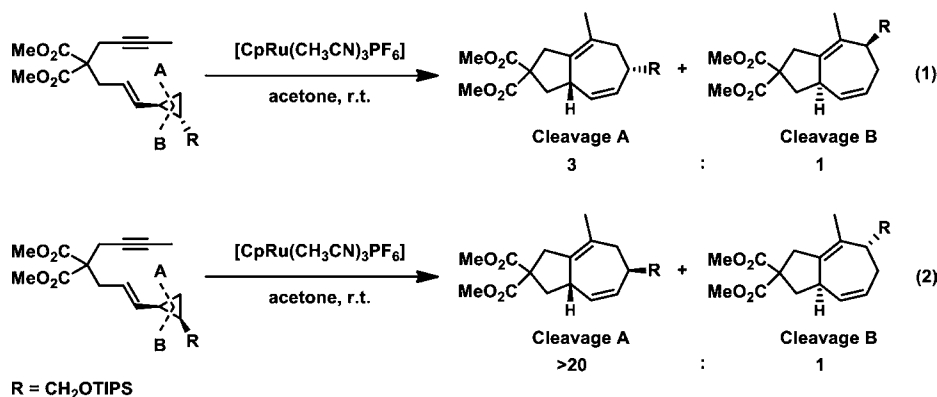
Scheme 3. Proposed Mechanisms for Transition-Metal-Catalyzed (5+2) Cycloadditions



Scheme 6. Selected Examples of Diastereoselectivities of Ru(II)-Catalyzed Intramolecular (5+2) Cycloaddition



Scheme 7. Selected Examples of Regioselectivities of Ru(II)-Catalyzed Intramolecular (5+2) Cycloaddition



transition-metal-catalyzed reactions, there is not a thorough understanding of such effects.

Diastereo- and regioselectivities are also intriguing: (1) The stereochemistry of allylic substituents in the tether strongly affects the created bridgehead stereogenic center. In all investigated cases, the allylic hydroxyl group is *trans* to the bridgehead hydrogen, and disubstitution on the allylic position increases the diastereoselectivity (Scheme 6). (2) The *trans*-1,2-disubstituted cyclopropane has a small preference to cleave the less substituted C–C bond, and the regioselectivity increases dramatically in the *cis*-disubstituted cyclopropane (Scheme 7). What are the origins of the diastereo- and regioselectivities? In order to understand the above questions, we used density functional theory (DFT) calculations to explore the mechanism, solvent effects, and the origins of selectivities involved in Ru(II)-catalyzed intramolecular (5+2) cycloadditions and ene reactions between vinylcyclopropanes and alkynes.

COMPUTATIONAL DETAILS

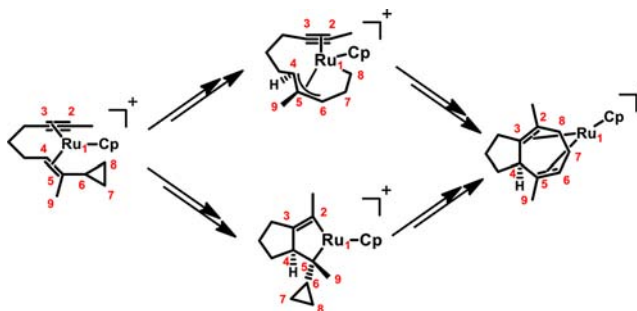
Geometry optimizations, frequencies, and thermal energy corrections were performed with the B3LYP functional, 6-31G(d) basis set for all main group elements and LANL2DZ basis set for ruthenium implemented in Gaussian 09.¹⁷ Energies were evaluated with the M06 method,¹⁸ 6-311+G(2d,p) basis set for all main group elements and LANL2DZ basis set for ruthenium. All reported free energies involve zero-point vibrational energy corrections and thermal corrections to Gibbs free energy at 298 K. The solvation free energy corrections were computed with the SMD model on gas-phase optimized geometries, and acetone was chosen as the solvent for

consistency with the experiment. Computed structures are illustrated using CYLVIEW drawings.¹⁹

RESULTS AND DISCUSSIONS

1. Mechanism. *1.1. Metallacyclohexene Pathway vs Metallacyclopentene Pathway.* To study the feasibility of metallacyclohexene and metallacyclopentene pathways, we first calculated the free energy profiles of both pathways starting from the substrate-coordinated complex to the seven-membered ring product-coordinated complex (atom labeling is shown in Scheme 8, detailed free energy profiles are provided in Figure 1, and optimized structures are shown in Figures 2 and 3).

Scheme 8. Metallacyclohexene and Metallacyclopentene Intermediates in Ru(II)-Catalyzed (5+2) Cycloaddition



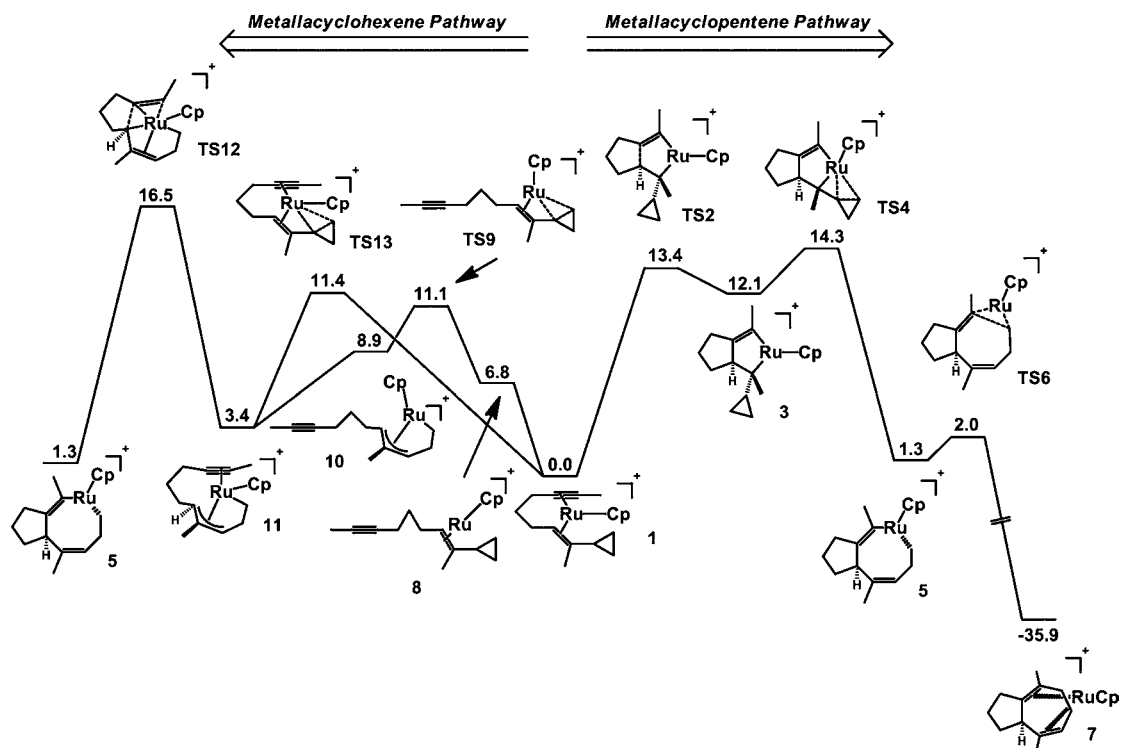


Figure 1. Free energy profiles of metallacyclohexene and metallacyclopentene pathways in Ru(II)-catalyzed (5+2) cycloaddition.

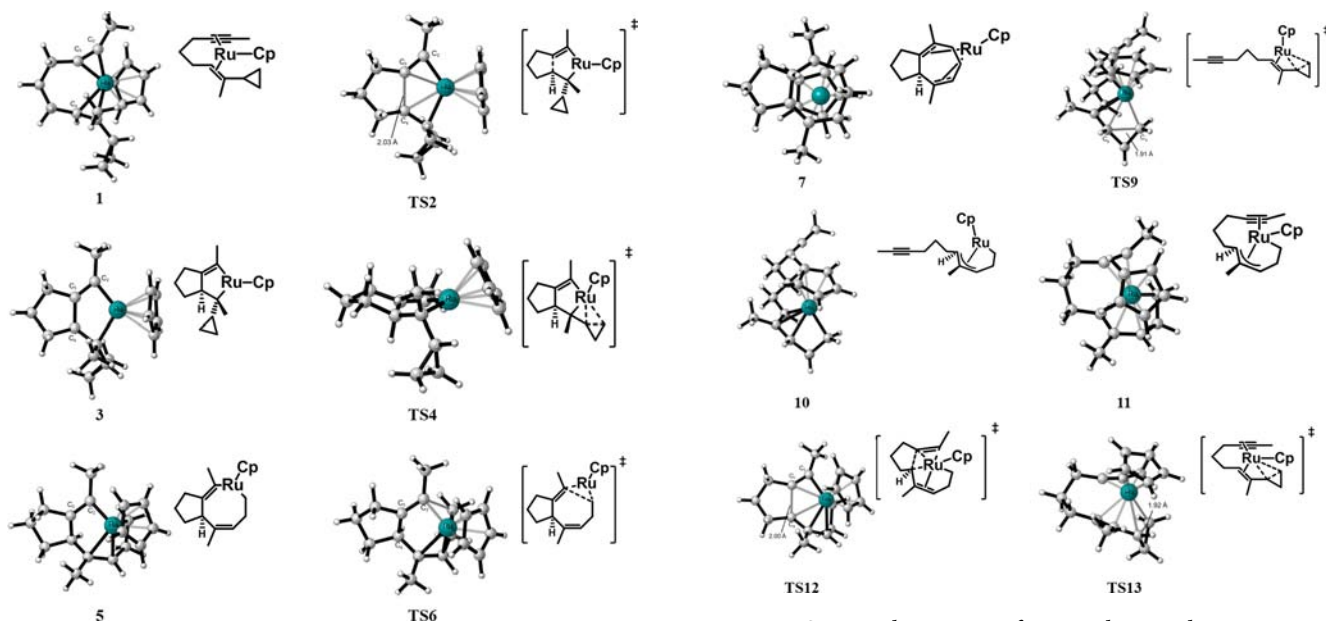


Figure 2. Optimized structures of intermediates and transition states in metallacyclohexene and metallacyclopentene pathways of Ru(II)-catalyzed (5+2) cycloaddition. All species have one positive charge.

Figure 3. Optimized structures of intermediates and transition states in metallacyclopentene and metallacyclohexene pathways of Ru(II)-catalyzed (5+2) cycloaddition. All species have one positive charge.

Complex **1** can undergo the metallacyclopentene pathway with an initial ene-yne oxidative cyclization via **TS2** (13.4 kcal/mol). From intermediate **3** (12.1 kcal/mol), the cyclopropane cleavage could occur with a 2.2 kcal/mol barrier (**TS4**) to give the ruthenacyclooctadiene intermediate **5** (1.3 kcal/mol). The overall barrier of ruthenacyclopentene pathway from complex **1** is 14.3 kcal/mol, and the rate-determining step is the cyclopropane cleavage step with **TS4**. This conclusion is consistent with the studies of the alkene-alkyne coupling

where formation of the ruthenacyclopentene is reversible and the product-determining step is the β -hydrogen insertion.¹³

Alternatively, the metallacyclohexene pathway can occur with an initial cyclopropane cleavage (Figure 1). The cyclopropane cleavage can proceed with or without the intramolecular alkyne coordination. With alkyne coordination, ruthenacyclohexene intermediate **11** (3.4 kcal/mol) can be formed via **TS13** (11.4 kcal/mol). Alternatively, the alkyne can dissociate from ruthenium first to give the intermediate **8** (6.8 kcal/mol). The electron-deficient ruthenium then catalyzes the cyclo-

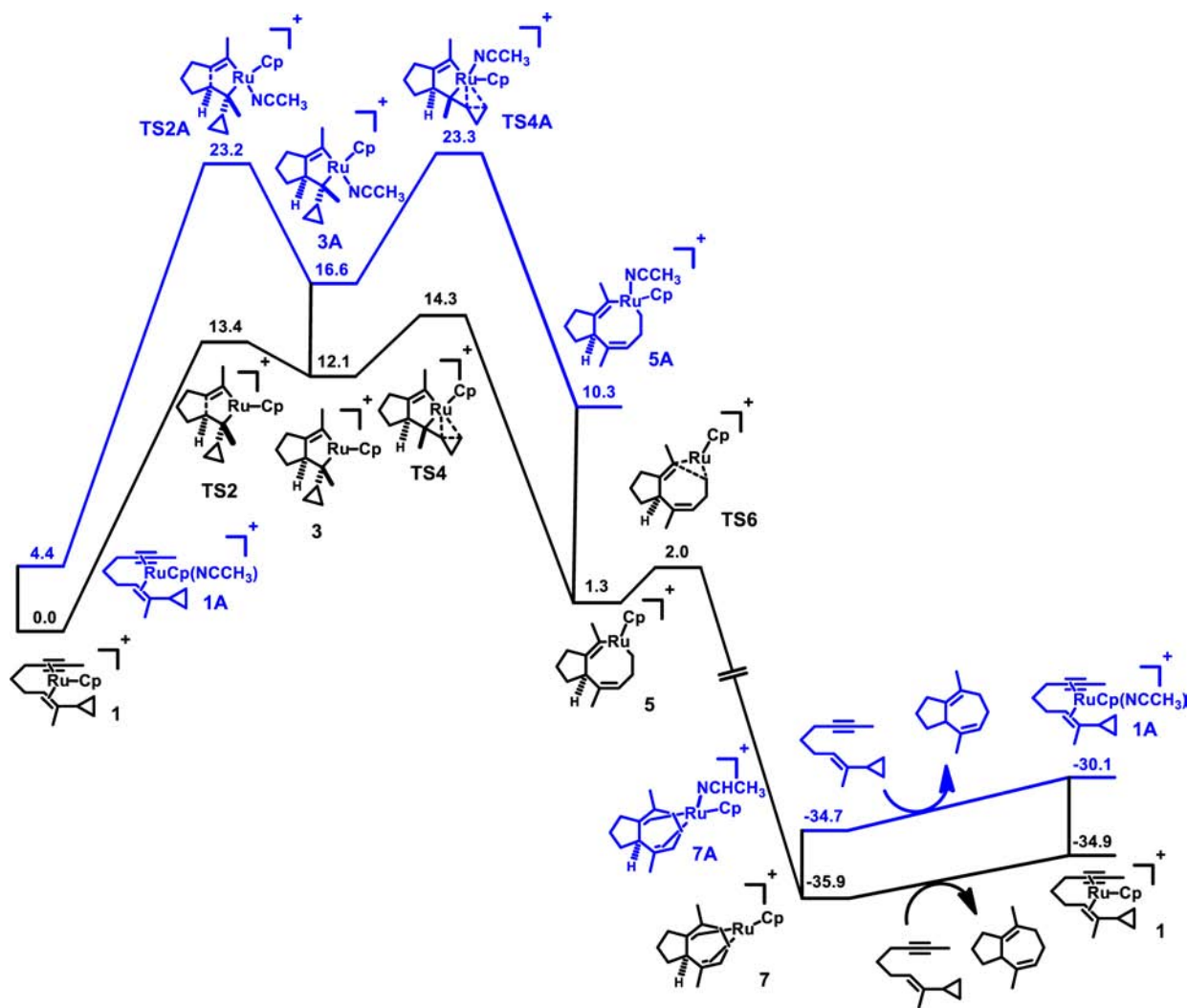


Figure 4. Free energy profiles of metallacyclopentene pathway with (blue) and without acetonitrile coordination (black) in Ru(II)-catalyzed intramolecular (5+2) cycloaddition with VCP and alkyne (in acetone).

propane cleavage through **TS9** (11.1 kcal/mol) to give the post-intermediate **10** (8.9 kcal/mol). Subsequently, the alkyne can coordinate to ruthenium again to generate the same ruthenacyclohexene intermediate **11**. Complex **11** will further undergo 2π insertion via **TS12** (16.5 kcal/mol) to give the same ruthenaoctadiene intermediate **5**. The metallacyclohexene pathway requires a 16.5 kcal/mol barrier, and the rate-determining step is the 2π insertion of alkyne.

Consistent with the Trost's experimental studies, the metallacyclopentene pathway is preferred by 2.2 kcal/mol. The two complexes, **1** (0.0 kcal/mol) and **11** (3.4 kcal/mol), are somewhat different in energy but have more similar reaction barriers (14.3 kcal/mol for **1** and 13.1 kcal/mol for **11**). Thus, the relative stabilities of **1** and **11** mainly lead to the small preference for the metallacyclopentene pathway, **1** to **TS2**. The preference for the metallacyclopentene pathway is in contrast to the rhodium catalyst, which significantly favors the metallacyclohexene pathway. The major difference between ruthenium and rhodium catalysts is the barrier difference between the 2π insertion of metallacyclohexene intermediate (**11** to **TS12**) and ene-yne oxidative cyclization of substrate-coordinated complex (**1** to **TS2**). With the rhodium catalyst,¹⁰ the 2π insertion step has a much lower barrier than the oxidative cyclization, while the two steps have very similar

barriers to those of the ruthenium catalyst. The origins of the barrier difference may lie in the differences in the redox potentials of different transition-metal catalysts. The oxidation state of the transition metal increases in the metallacycle formation but remains the same in the 2π insertion. Therefore, the metal complex that has a lower oxidation potential should favor the ene-yne oxidative cyclization.²⁰

1.2. Acetonitrile Coordination and Solvent Effects. The possibility of acetonitrile coordination to the ruthenium catalyst was also studied. Figure 4 shows the free energy profiles for the reaction with only Cp as the ligand (black) and with additional acetonitrile coordination (blue). The optimized structures are provided in Figure 5. All the acetonitrile-coordinated intermediates and transition states either have higher energies than in the absence of acetonitrile or cannot be located (**TS6A**).²¹ In addition, the acetone coordination is even less favorable than the acetonitrile coordination.²² Because the DFT calculations tend to overestimate the energy contribution from solvation entropy, the relative stability between **1** and **1A** is not conclusive based on the 4.4 kcal/mol free energy difference. Although the real structure of substrate-coordinated complex is still in question, we believe the reaction will follow the pathway with only Cp as the ligand because of the large energy difference between **TS4** and **TS4A**. Therefore, all three

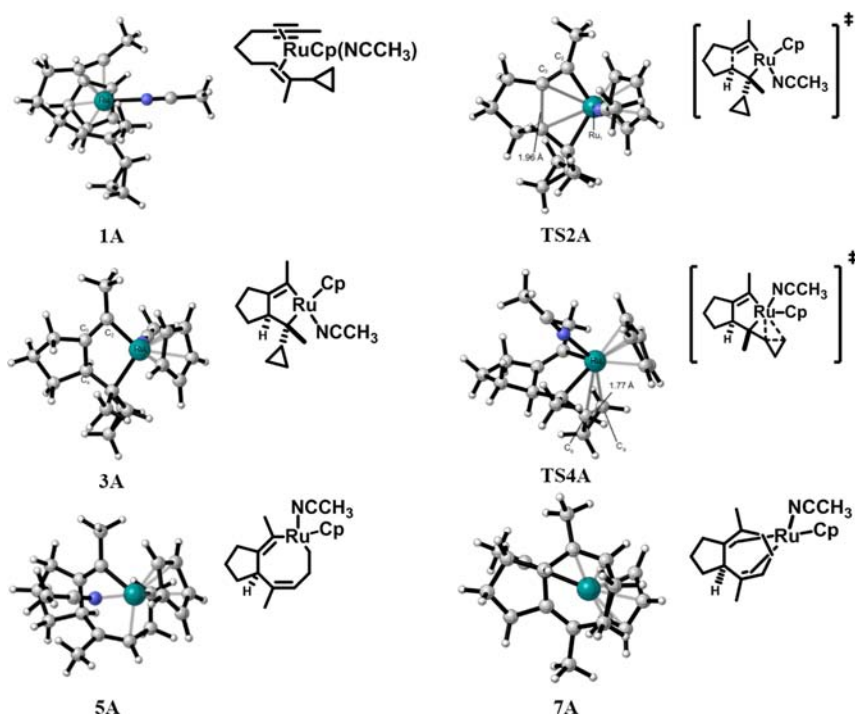
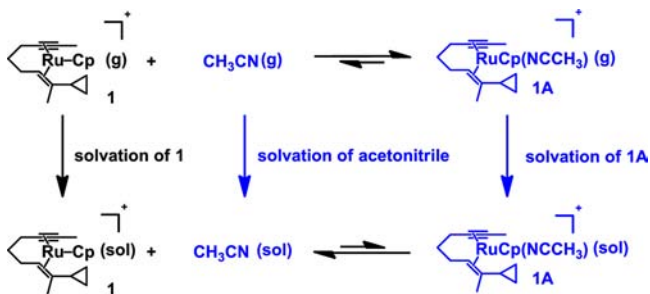


Figure 5. Optimized structures of intermediates and transition states with additional acetonitrile coordination in metallacyclopentene pathways of Ru(II)-catalyzed intramolecular (5+2) cycloaddition. All species have one positive charge.

acetonitriles in the precatalyst will dissociate to achieve the reaction.

There are strong ruthenium–acetonitrile bonds in the optimized structures (the bond distances varies between 2.08 and 2.23 Å), and acetonitrile coordination is favorable in the gas phase. Scheme 9 gives an analysis of the thermodynamics of

Scheme 9. Thermodynamic Equilibrium of Acetonitrile Coordination of Ruthenium Complexes Involved in Ru(II)-Catalyzed Intramolecular (5+2) Cycloaddition in Gas Phase and Solution



acetonitrile coordination at equilibrium. Because the pre- and post-coordination complexes have similar polarities, the difference of solvation energies between **1** (52.4 kcal/mol) and **1A** (50.1 kcal/mol) is only 2.3 kcal/mol. The major contributor to the equilibrium preference between the gas phase and solvent comes from the solvation energy of acetonitrile (6.8 kcal/mol). The solvation energy of acetonitrile is very strong in acetone and alters the complexation equilibrium and the reaction barriers. Therefore, we also calculated the free energy profiles with acetonitrile-coordinated ruthenium complex in the gas phase (shown in Figure 6).

In the gas phase, acetonitrile coordination is favorable and the intermediates are more stabilized than the transition states.

The reaction pathway without the acetonitrile coordination requires a 16.7 kcal/mol overall barrier, which is similar to the barrier in acetone. With the acetonitrile coordination, the barrier increases to 23.4 kcal/mol (from **7A** to **TS4A**) due to the significant stabilization of the resting state **7A**. Compared to the acetone solvent, the gas phase can be considered as an extreme of nonpolar solvent, and the difference in free energy profiles between gas phase and acetone solvent explains the origin of the superior solvent effect of acetone in this reaction. The polar solvent acetone facilitates acetonitrile dissociation from the precatalyst, which destabilizes the resting state and lowers the overall reaction barrier. In a nonpolar solvent, acetonitrile coordination is favorable and stabilizes the resting states of the catalytic cycle, resulting in a higher reaction barrier and lower efficiency.

2. Origins of Selectivity in Competition between (5+2) Cycloaddition and Ene Reaction. *2.1. trans-VCP.* As noted earlier, the *trans*-VCP substrate gives mainly (5+2) cycloaddition involving the ring-opening of the cyclopropane (Scheme 5). The *cis*-VCP produces mainly ene product, but some of the (5+2) product is formed as well. This seems obvious from the structure of substrate, but it should be noted that the intermediates involved from the *trans* vs *cis* substrates are diastereomeric. In order to explore the origins of such selectivity in more detail, we first calculated the free energy profiles for both (5+2) cycloaddition and ene reaction with *trans*-VCP (shown in Figure 7).

The ruthenacyclopentene intermediate **3** (12.1 kcal/mol) can undergo cyclopropane cleavage via **TS4**; this requires only a 2.2 kcal/mol barrier. The ruthenacyclooctadiene intermediate **5** (1.3 kcal/mol) then generates the seven-membered ring product through a facile reductive elimination via **TS6** (2.0 kcal/mol). Alternatively, β -hydride elimination can occur in the intermediate **3** initiated by an agostic intermediate **15** (13.5 kcal/mol) via **TS14** (17.2 kcal/mol). Then β -hydride

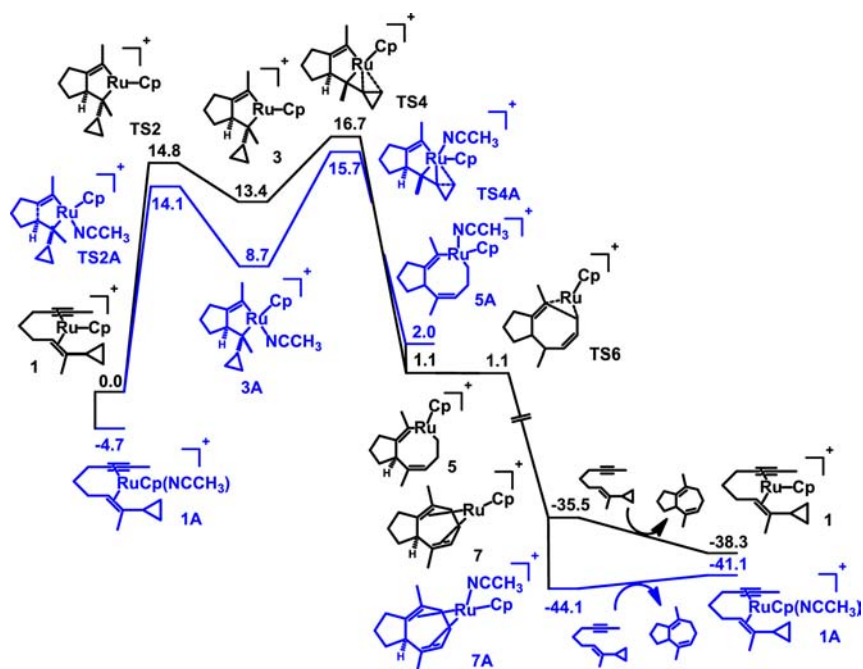


Figure 6. Free energy profiles of metallacyclopentene pathway with (blue) and without acetonitrile coordination (black) in Ru(II)-catalyzed (S+2) cycloaddition (gas phase).

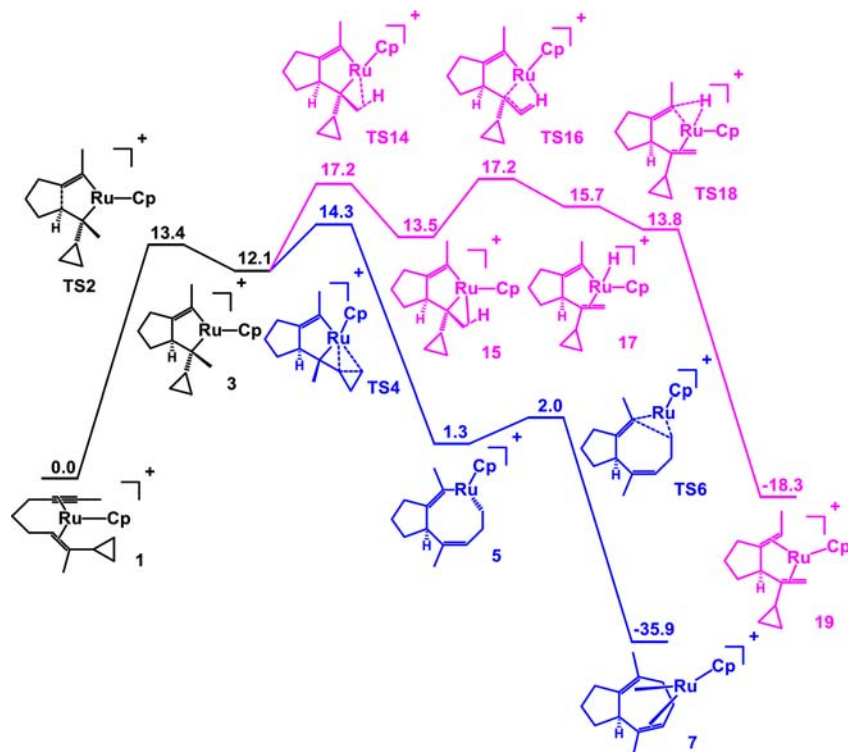


Figure 7. Free energy profiles of reductive elimination (blue) and β -hydride elimination (pink) in Ru(II)-catalyzed (S+2) cycloaddition with *trans*-VCP.

elimination through TS16 gives the intermediate 17 (15.7 kcal/mol). Finally, the diene complex 19 can be formed via C–H reductive elimination. For β -hydride elimination, both TS14 and TS16 are rate-determining and require 5.1 kcal/mol barriers from the intermediate 3.

The calculations predict a preference for (S+2) cycloaddition in *trans*-VCP, as is found experimentally. The

difference between TS4 and TS14 explains the origins of selectivity; these transition structures are shown in Figure 8. Cyclopropane cleavage (TS4) is favored intrinsically. To achieve the Ru₁–H₁₀ bond interaction and form an agostic intermediate, the methyl group must rotate to a larger degree in TS14, resulting in an unfavorable distortion and higher energy of TS14 compared to TS4.

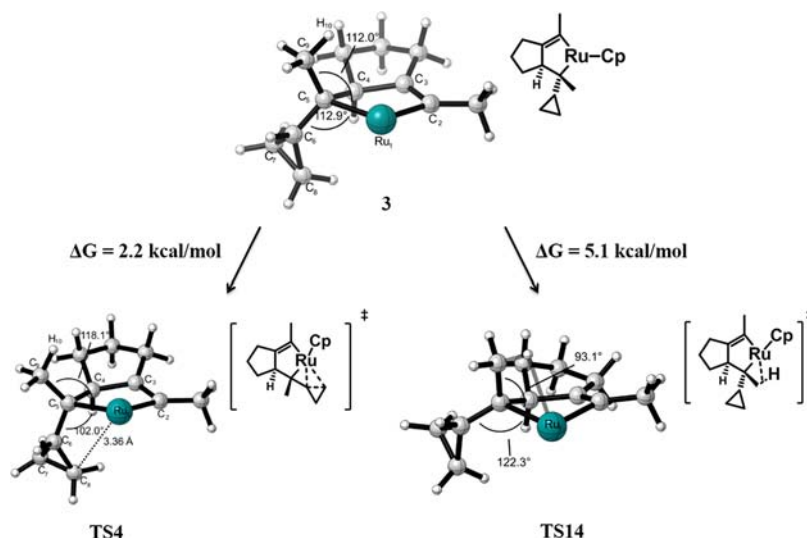


Figure 8. Free energies and structures of selectivity-determining transition states in *trans*-VCP. The Cp ligand is not shown for clarity, and all species have one positive charge.

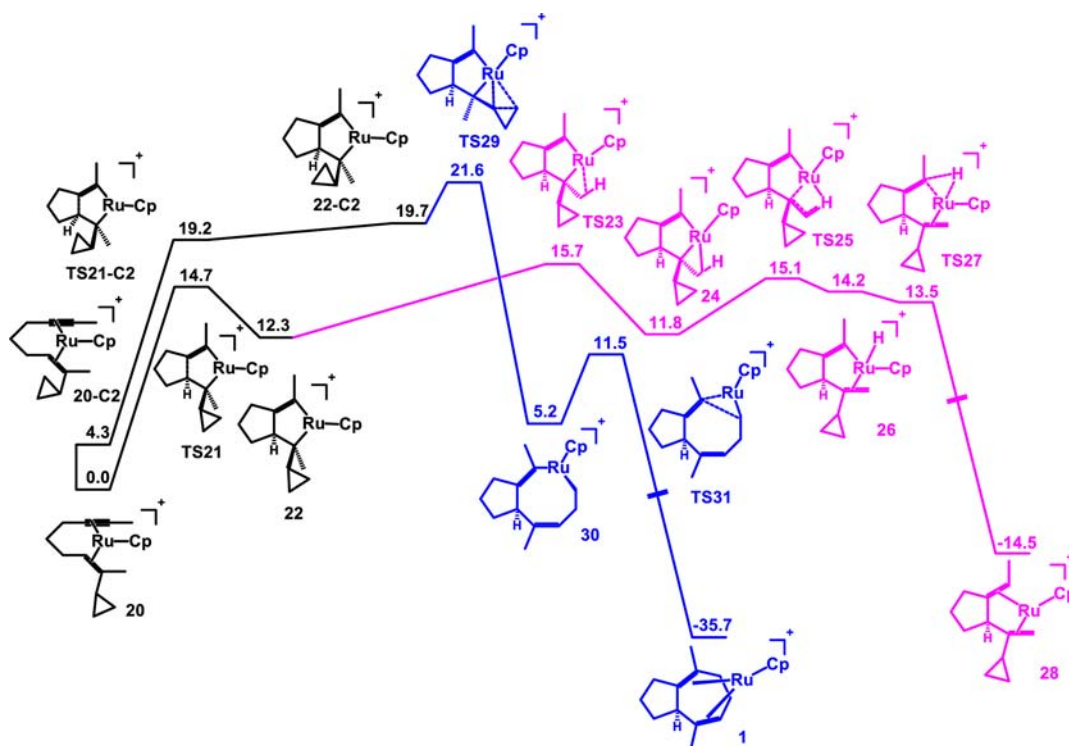
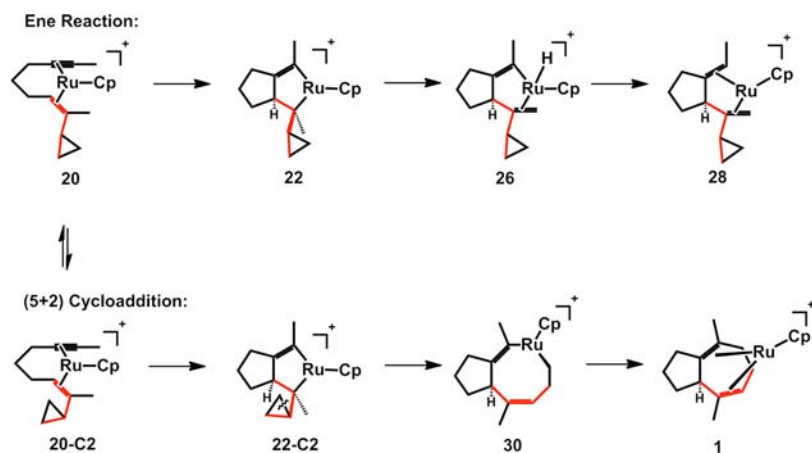


Figure 9. Free energy profiles of reductive elimination (blue) and β -hydride elimination (pink) in Ru(II)-catalyzed (5+2) cycloaddition with *cis*-VCP.

2.2. *cis*-VCP. Subsequently, the origin of selectivity of *cis*-VCP was also studied. Here, β -hydride elimination has a lower barrier, and the ene product is preferred (free energy profile is shown in Figure 9). The key difference between *trans*- and *cis*-VCP is the position of the cyclopropyl group. The favored conformation of ruthenacyclopentene intermediate **22** in *cis*-VCP requires rotation of the cyclopropyl group in order to form a *cis*-double bond in the cycloheptadiene (shown in Scheme 10). This rotation is not necessary for β -hydride elimination. Therefore, for *cis*-VCP, the (5+2) cycloaddition and ene reaction start from different intermediates (**20** and **20-C2** in Scheme 8 and Figure 9).

The ene reaction pathway of *cis*-VCP is similar to that of *trans*-VCP. The rate-determining step is from **TS23** to form the agostic intermediate **24**, which requires an overall barrier of 15.7 kcal/mol. For the (5+2) cycloaddition, the intermediate **20** has to adopt an unfavorable conformation, **20-C2**, in order to generate the *cis*-double bond in the cycloheptadiene. After oxidative cyclization, the formed intermediate, **22-C2** (19.7 kcal/mol), is much less stable than the favored conformation **22** (12.3 kcal/mol).²³ This instability is due to steric repulsion between the formed five-membered ring and the cyclopropyl group, which are shown by the H–H distance and the Newman projection of C5–C6 (Figure 10). Therefore, although the

Scheme 10. Key Intermediates of (5+2) Cycloaddition and Ene Reaction with *cis*-VCP Substrate^a

^aThe carbons in one of the *cis*-double bonds of cycloheptadiene are labeled in red.

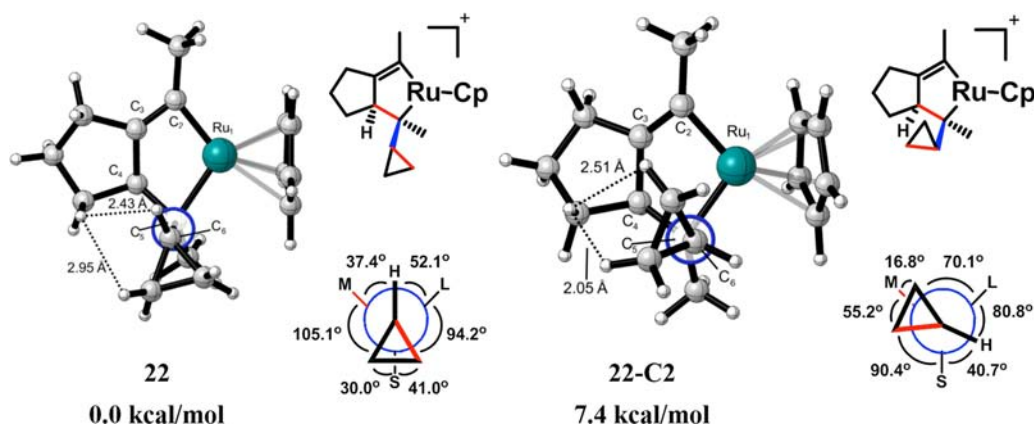
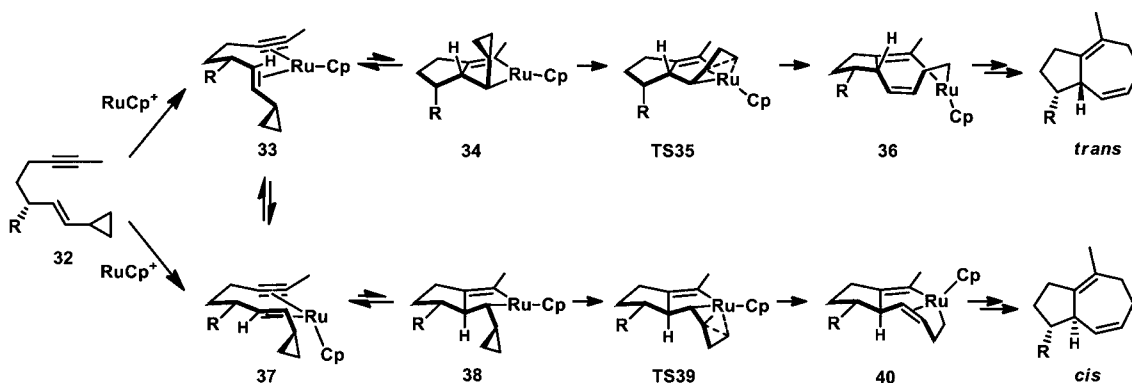


Figure 10. Optimized structures, Newman projection of C5–C6, and relative Gibbs free energies of intermediate 22 and 22-C2. S stands for the methyl group, M stands for the formed five-membered carbocycle, and L stands for the ruthenium.

Scheme 11. Reaction Pathways That Generate the *trans*- and *cis*-Diastereomers of Ru(II)-Catalyzed (5+2) Cycloaddition

cyclopropane cleavage still has a lower intrinsic barrier (1.9 kcal/mol from 22-C2 to TS29) compared to β -hydride elimination (3.4 kcal/mol from 22 to TS23), the relative stabilities of 22 and 22-C2 overruled the intrinsic barrier differences and led to the β -hydride elimination and ene reaction eventually.

3. Origins of Diastereo- and Regioselectivities.

3.1. Diastereoselectivities. As noted earlier, the stereochemistry of allylic substituents in the tether strongly affects the formed bridgehead stereogenic center. The allylic hydroxyl

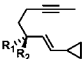
group is *trans* to bridgehead hydrogen, and disubstitution on the allylic position dramatically increases the diastereoselectivities (Scheme 6). In order to explore the origins of the diastereoselectivities, we studied the reaction pathways that generate the diastereomeric (5+2) cycloadducts.

Scheme 11 shows the key intermediates and transition states that generate the diastereoselectivities. From enantiopure substrate 32, substrate–catalyst complex 33 undergoes oxidative cyclization to form the bicyclic post-intermediate 34 with the substituent R *trans* to the bridgehead hydrogen.

Subsequent irreversible cyclopropane cleavage via TS35 generates the eight-membered ring intermediate **36** and eventually the (5+2) cycloadduct with R *trans* to the bridgehead hydrogen. In the *cis*-pathway, the diastereomeric substrate–catalyst complex **37** generates the post-intermediate **38** with the allylic substituent R *cis* to the bridgehead hydrogen. Subsequent cyclopropane cleavage produces the eight-membered ring intermediate **40** through TS39 and eventually the (5+2) cycloadduct with R *cis* to the bridgehead hydrogen.

Table 1 shows the free energies of the intermediates and transition states from Scheme 11 with various allylic

Table 1. Gibbs Free Energies of Key Intermediates and Transition States That Generate the *trans*- and *cis*-Diastereomeric Cycloadducts in Ru(II)-Catalyzed (5+2) Cycloadditions with Various Allylic Substituents

entry		<i>trans</i>			<i>cis</i>			$\Delta\Delta G(\text{TS35-TS39})$
		33	34	TS35	37	38	TS39	
1	R ₁ =Me;R ₂ =H	0.0	14.6	16.4	3.0	13.0	15.0	+1.4
2	R ₁ =OH;R ₂ =H	0.0	12.3	14.5	2.3	12.9	15.0	-0.5
3	R ₁ =OH;R ₂ =Me	0.0	10.9	13.8	4.1	13.3	16.1	-2.3

substituents. In the case that the allylic position is monosubstituted by a methyl group, the *trans* cycloadduct is disfavored by 1.4 kcal/mol (Table 1, entry 1). Because the cyclopropane cleavage barriers are very similar in *trans* and *cis* pathways (1.8 kcal/mol from **34-1** to TS35-1 and 2.0 kcal/mol from **38-1** to TS39-1), the relative stabilities of **34-1** and **38-1** determine the diastereoselectivity. As shown in Figure 11, **34-1** has steric repulsion between the methyl substituent and its β -hydrogen from the double bond, while no such repulsion is

presented in **38-1** (shown in Figure 11). Therefore, steric effects lead to the preference for the *cis*-(5+2) cycloadduct when there is one allylic substituent.

In contrast, the *trans*-cycloadduct is favored with allylic hydroxyl substituents. The predicted preference is consistent with the experimental diastereoselectivities. When substituted with one hydroxyl group, **34-2** (12.3 kcal/mol) is 0.6 kcal/mol less stable than **38-2** (12.9 kcal/mol) (Table 1, entry 2). The origins of the reversed stabilities and diastereoselectivities are electrostatic interactions. The oxygen in **34-2** is closer to the cationic catalyst center, and thus the electrostatic stabilization from oxygen lone pairs makes **34-2** more stable. Furthermore, when the allylic position is disubstituted with methyl and hydroxyl groups, both electrostatic and steric interactions favor the *trans*-(5+2) cycloadduct and produce a higher diastereoselectivity. In **34-3**, the oxygen lone pairs provide stabilization similar to that in **34-2**, and the methyl substituent in **38-3** has steric repulsions with its β -hydrogen from the double bond. Therefore, the combined electrostatic and steric effects generate the higher diastereoselectivity observed in experiments.

3.2. Regioselectivities. The origins of regioselectivities are also studied. The reaction pathways that generate the regioselectivities are very similar to the reaction pathways that generate the diastereoselectivities (Scheme 12). From *trans*-1,2-disubstituted cyclopropane substrate **41**, substrate–catalyst complex **42** undergoes reversible oxidative cyclization to form the bicyclic post-intermediate **43**. Subsequent cyclopropane cleavage via TS44 produces the eight-membered ring intermediate **45** and eventually the (5+2) cycloadduct with the less substituted C–C bond cleaved (cleavage A). Alternatively, the substrate–catalyst complex **46** can follow a similar pathway to have the more substituted C–C bond cleaved (cleavage B), and the determining transition state is TS48.

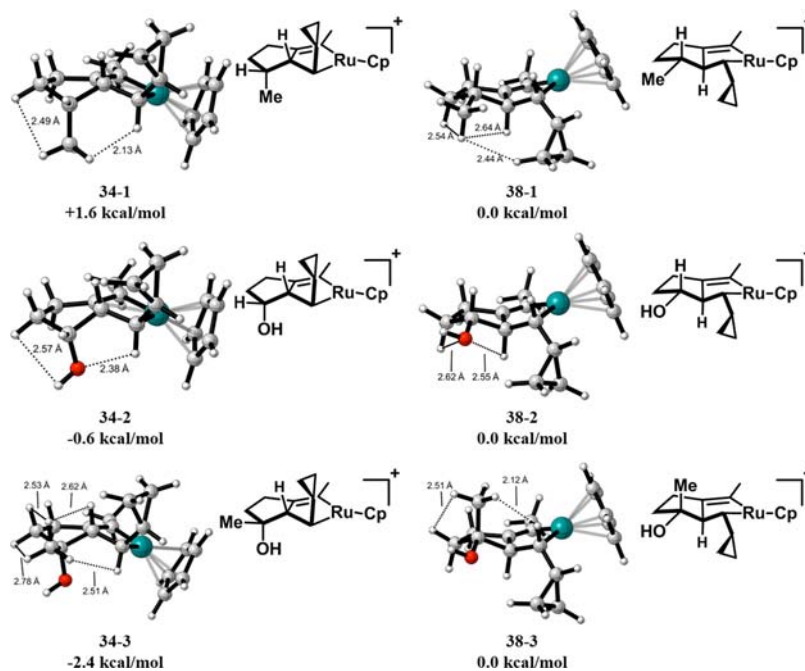


Figure 11. Optimized structures and relative Gibbs free energies of diastereomeric oxidative cyclization post-intermediates with various allylic substituents in Ru(II)-catalyzed (5+2) cycloaddition.

Scheme 12. Reaction Pathways That Cleave the More and Less Substituted C–C Bond of 1,2-Disubstituted Cyclopropane in Ru(II)-Catalyzed (5+2) Cycloaddition

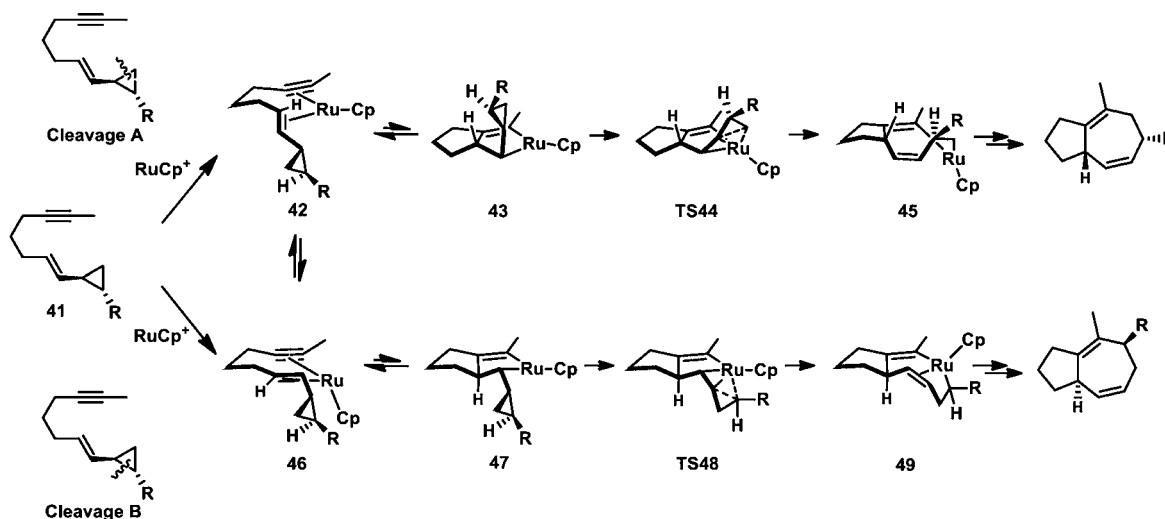


Table 2 shows the free energies of the intermediates and transition states from Scheme 12 with *trans*- and *cis*-1,2-

Table 2. Gibbs Free Energies of Key Intermediates and Transition States That Undergo the Cleavage A and Cleavage B Pathways in Ru(II)-Catalyzed (5+2) Cycloadditions with *trans*- and *cis*-1,2-Disubstituted Cyclopropanes

entry	substrate	Cleavage A			Cleavage B			$\Delta\Delta G(\text{TS44-TS48})$
		42	43	TS44	46	47	TS48	
1		0.0	14.1	17.4	2.4	14.0	16.8	+0.6
2		0.0	16.6	19.6	6.4	16.9	22.2	-2.6

disubstitution. With *trans*-disubstitution (Table 1, entry 1), the cleavages A and B have very similar barriers, and the experimental regioselectivity is low (Scheme 7). Figure 12 shows the optimized structures of the regioselectivity-determining transition states. In TS44-1 and TS48-1, the methyl substituent has no significant steric repulsion and is away from the reaction center in both cases; thus, cleavage A and cleavage B have very similar barriers and the regioselectivity is low. In contrast, the *cis*-disubstituted cyclopropane favors cleavage A dramatically. The methyl substituent in TS44-2 is still away from the reaction center, and the cyclopropane cleavage barrier of cleavage A is low (3.0 kcal/mol). However, the methyl substituent in TS48-2 is in a very sterically hindered position and close to the reaction center. Therefore, steric repulsion from the methyl substituent increases the barrier of cleavage B to 5.3 kcal/mol and generates higher regioselectivity in *cis*-1,2-disubstituted cyclopropane.

CONCLUSIONS

The mechanism and solvent effects of Ru(II)-catalyzed intramolecular (5+2) cycloaddition and ene reaction have been studied theoretically. The favored catalytic cycle involves an initial oxidative cyclization to produce a metallacyclopentene intermediate. Subsequent cyclopropane cleavage and C–C reductive elimination yield the (5+2) seven-membered ring product, while β -hydride elimination and C–H reductive elimination give the ene product. Acetone solvent is found to facilitate acetonitrile dissociation from the precatalyst and destabilize the resting state, resulting in a lower reaction barrier. Quite noteworthy are the complementary mechanisms for the (5+2) cycloaddition between rhodium and ruthenium catalysis. Such a mechanistic dichotomy offers the opportunity to modulate the selectivity and reactivity for any given substrate by simply changing the metal catalyst, which highlights the power of transition metal catalysis.

The origins of the reversed selectivity between (5+2) cycloaddition and ene reaction with *trans*- and *cis*-VCP were also revealed. In *trans*-VCP, the intrinsic lower barrier of cyclopropane cleavage leads to the seven-membered ring major product. *cis*-VCP requires an unfavorable rotation of the cyclopropyl group in order to generate the *cis*-double bond in the seven-membered ring product. This unfavorable rotation reverses the selectivity.

The origins of the diastereo- and regioselectivities have also been discovered. When the allylic position is substituted by a hydroxyl group, the oxygen lone pair provides stabilizing electrostatic interactions with the cationic catalyst center in one diastereomer, and the favored diastereomer has the hydroxyl group *trans* to the bridgehead hydrogen. The origins of regioselectivities are steric repulsions. In the *trans*-1,2-disubstituted cyclopropane, cleavages of both the more and less substituted C–C bond of the cyclopropane have no significant steric repulsions from the substituent. In contrast, the methyl substituent of the *cis*-1,2-disubstituted cyclopropane causes much steric repulsion in the transition state that cleaves the more substituted C–C bond, and thus a higher regioselectivity is found.

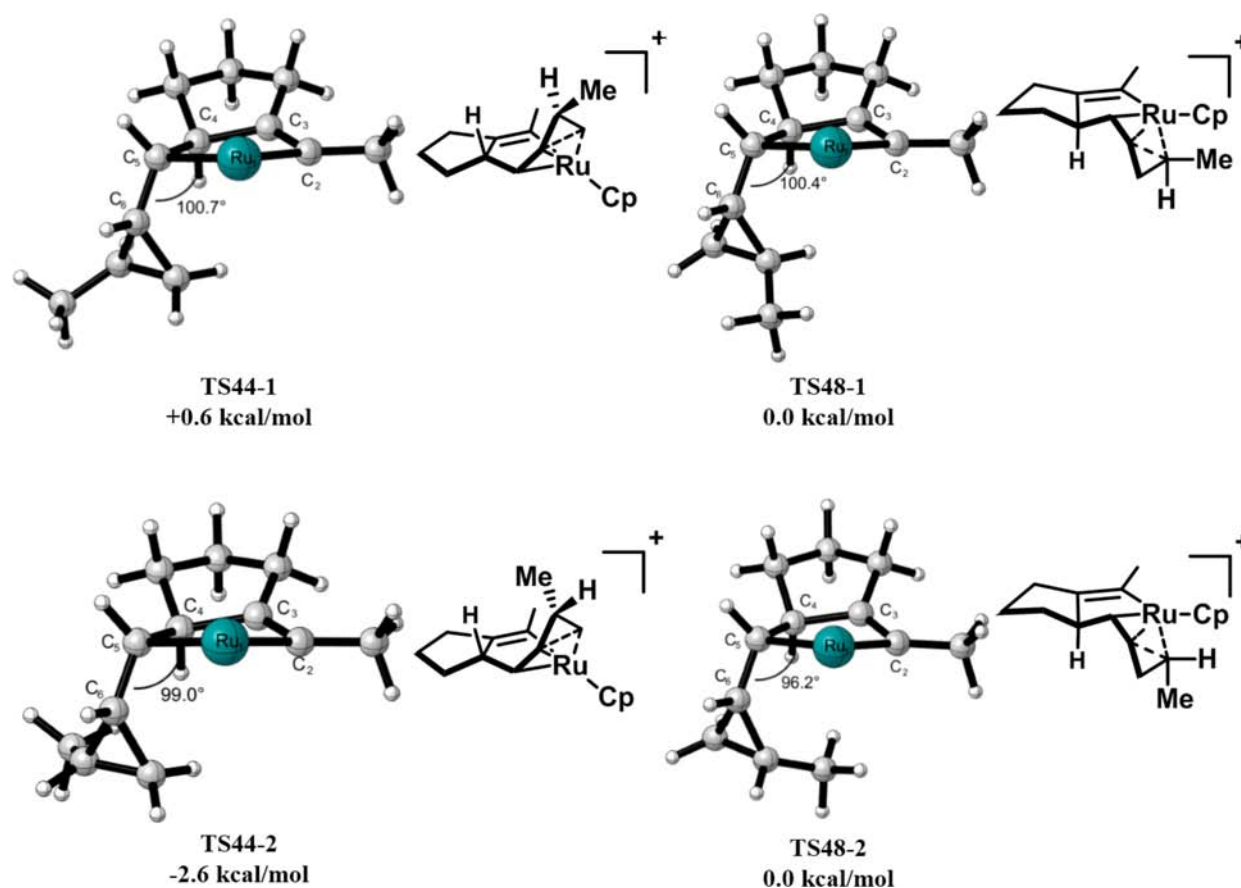


Figure 12. Optimized structures and relative Gibbs free energies of cyclopropane cleavage transition states in Ru(II)-catalyzed (5+2) cycloaddition with *trans*- and *cis*-1,2-disubstituted cyclopropanes. Cyclopentadienyl ligand is not shown for clarity, and TS44-1 and TS44-2 are the mirror images of their real structures.

■ ASSOCIATED CONTENT

📄 Supporting Information

Optimized Cartesian coordinates and energies, Gibbs free energies and optimized structures of acetone-coordinated intermediates in the metallacyclopentene pathway, and complete ref 17. This material is available free of charge via the Internet at <http://pubs.acs.org>.

■ AUTHOR INFORMATION

Corresponding Author

houk@chem.ucla.edu; bmtrout@stanford.edu

Notes

The authors declare no competing financial interest.

■ ACKNOWLEDGMENTS

We thank Dr. Peng Liu for helpful discussions. We are grateful to the National Science Foundation (CHE-0548209 and CHE-0948222) for financial support of this research. Calculations were performed on the Hoffman2 cluster at UCLA and the Extreme Science and Engineering Discovery Environment (XSEDE), which is supported by the NSF.

■ REFERENCES

(1) (a) Wender, P. A.; Fuji, M.; Husfeld, C. O.; Love, J. A. *Org. Lett.* **1999**, *1*, 137. (b) Wender, P. A.; Zhang, L. *Org. Lett.* **2000**, *2*, 2323. (c) Trost, B. M.; Shen, H. C.; Surivet, J. P. *Angew. Chem., Int. Ed.* **2003**, *42*, 3943. (d) Padwa, A.; Boonsombat, J.; Rashatasakhon, P.; Willis, J. *Org. Lett.* **2005**, *7*, 3725. (e) Nakamura, S.; Sugano, Y.; Kikuchi, F.;

Hashimoto, S. *Angew. Chem., Int. Ed.* **2006**, *45*, 6532. (f) Battiste, M. A.; Pelphey, P. M.; Wright, D. L. *Chem.—Eur. J.* **2006**, *12*, 3438. (g) Trost, B. M.; Hu, Y.; Horne, D. B. *J. Am. Chem. Soc.* **2007**, *129*, 11781. (h) Trost, B. M.; Waser, J.; Meyer, A. *J. Am. Chem. Soc.* **2008**, *130*, 16424. (i) Butenschön, H. *Angew. Chem., Int. Ed.* **2008**, *47*, 5287. (j) Shimada, N.; Hanari, T.; Kurosaki, Y.; Takeda, K.; Anada, M.; Nambu, H.; Shiro, M.; Hashimoto, S. *J. Org. Chem.* **2010**, *75*, 6039. (k) Wender, P. A.; Lesser, A. B.; Sirois, L. E. *Org. Synth.* **2011**, *88*, 109. (2) (a) Kantorowski, E. J.; Kurth, M. J. *Tetrahedron* **2000**, *56*, 4317. (b) Byrne, L. A.; Gilheany, D. G. *Synlett* **2004**, *6*, 933. (c) Matsuda, T.; Makino, M.; Murakami, M. *Angew. Chem., Int. Ed.* **2005**, *44*, 4608. (d) Tite, T.; Tsimilaza, A.; Lallemand, M.; Tillequin, F.; Leproux, P.; Libot, F.; Husson, H. *Eur. J. Org. Chem.* **2006**, 863. (e) Hashimoto, T.; Naganawa, Y.; Maruoka, K. *J. Am. Chem. Soc.* **2009**, *131*, 6614. (f) Laventine, D. L.; Cullis, P. M.; Garcia, M. D.; Jenkins, P. R. *Tetrahedron Lett.* **2009**, *50*, 3657. (g) Yadav, D. B.; Morgans, G. L.; Aderibigbe, B. A.; Madeley, L. G.; Fernandes, M. A.; Michael, J. P.; de Koning, C. B.; van Otterlo, W. A. L. *Tetrahedron* **2011**, *67*, 2991. (h) Pulido, F. J.; Barbero, A.; Castreño, P. *J. Org. Chem.* **2011**, *76*, 5850. (i) Cao, H.; Vieira, T. O.; Alper, H. *Org. Lett.* **2011**, *13*, 11. (j) Li, X.; Zhang, M.; Shu, D.; Robichaux, P. J.; Huang, S.; Tang, W. P. *Angew. Chem., Int. Ed.* **2011**, *50*, 10421. (k) Usanov, D. L.; Yamamoto, H. *Org. Lett.* **2012**, *14*, 414. (3) (a) Yet, L. *Chem. Rev.* **2000**, *100*, 2963. (b) Wender, P. A.; Croatt, M. P.; Deschamps, N. M. In *Comprehensive Organometallic Chemistry III*; Crabtree, R. H., Mingos, D. M. P., Eds.; Elsevier: Oxford, 2007; Vol. 10, pp 603–647. (4) For reviews, see: (a) Wender, P. A.; Love, J. A. In *Advances in Cycloaddition*; JAI Press: Greenwich, CT, 1999; Vol. 5, pp 1–45. (b) Wender, P. A.; Gamber, G. G.; Williams, T. J. In *Modern Rhodium-*

Catalyzed Organic Reactions; Wiley-VCH: Weinheim, 2005; pp 263–299. See also refs 1g and 3b.

(5) For the first report by Wender, see: (a) Wender, P. A.; Takahashi, H.; Witulski, B. *J. Am. Chem. Soc.* **1995**, *117*, 4720. For intermolecular reactions involving alkynes, see: (b) Wender, P. A.; Rieck, H.; Fujii, M. *J. Am. Chem. Soc.* **1998**, *120*, 10976. (c) Wender, P. A.; Dyckman, A. J.; Husfeld, C. O.; Scanio, M. J. C. *Org. Lett.* **2000**, *2*, 1609. (d) Wender, P. A.; Barzilay, C. M.; Dyckman, A. J. *J. Am. Chem. Soc.* **2001**, *123*, 179. (e) Wender, P. A.; Gamber, G. G.; Scanio, M. J. C. *Angew. Chem., Int. Ed.* **2001**, *40*, 3895. (f) Wender, P. A.; Stemmler, R. T.; Sirois, L. E. *J. Am. Chem. Soc.* **2010**, *132*, 2532. (g) Wender, P. A.; Sirois, L. E.; Stemmler, R. T.; Williams, T. J. *Org. Lett.* **2010**, *12*, 1604. For intermolecular reactions involving allenes, see: (h) Wegner, H. A.; de Meijere, A.; Wender, P. A. *J. Am. Chem. Soc.* **2005**, *127*, 6530. For Ni- and Fe-catalyzed (5+2) cycloadditions, see: (i) Zuo, G.; Louie, J. *J. Am. Chem. Soc.* **2005**, *127*, 5798. (j) Fürstner, A.; Majima, K.; Martin, R.; Krause, H.; Kattinig, E.; Goddard, R.; Lehmann, C. W. *J. Am. Chem. Soc.* **2008**, *130*, 1992.

(6) (a) Wender, P. A.; Fujii, M.; Husfeld, C. O.; Love, J. A. *Org. Lett.* **1999**, *1*, 137. (b) Wender, P. A.; Zhang, L. *Org. Lett.* **2000**, *2*, 2323. (c) Wender, P. A.; Bi, F. C.; Brodney, M. A.; Gosselin, F. *Org. Lett.* **2001**, *3*, 2105. (d) Ashfeld, B. L.; Martin, S. F. *Tetrahedron* **2006**, *62*, 10497–10506. (e) Jiao, L.; Yuan, C.; Yu, Z.-X. *J. Am. Chem. Soc.* **2008**, *130*, 4421. (f) Yuan, C.; Jiao, L.; Yu, Z.-X. *Tetrahedron Lett.* **2010**, *51*, 5674. (g) Liang, Y.; Jiang, X.; Yu, Z.-X. *Chem. Commun.* **2011**, *47*, 6659. (h) Liang, Y.; Jiang, X.; Fu, X.-F.; Ye, S.-Y.; Wang, T.; Yuan, J.; Wang, Y.; Yu, Z.-X. *Chem. Asian J.* **2012**, *7*, 593. See also refs 1g, 1h, and 14c.

(7) (a) Wender, P. A.; Gamber, G. G.; Hubbard, R. D.; Zhang, L. *J. Am. Chem. Soc.* **2002**, *124*, 2876. (b) Wang, Y.; Wang, J.; Su, J.; Huang, F.; Jiao, L.; Liang, Y.; Yang, D.; Zhang, S.; Wender, P. A.; Yu, Z.-X. *J. Am. Chem. Soc.* **2007**, *129*, 10060. (c) Huang, F.; Yao, Z.-K.; Wang, Y.; Wang, Y.; Zhang, J.; Yu, Z.-X. *Chem. Asian J.* **2010**, *5*, 1555.

(8) Wender, P. A.; Gamber, G. G.; Hubbard, R. D.; Pham, S. M.; Zhang, L. *J. Am. Chem. Soc.* **2005**, *127*, 2836.

(9) (a) Jiao, L.; Ye, S.-Y.; Yu, Z.-X. *J. Am. Chem. Soc.* **2008**, *130*, 7178. (b) Jiao, L.; Lin, M.; Yu, Z.-X. *Chem. Commun.* **2010**, *46*, 1059.

(10) Jiang, G.-J.; Fu, X.-F.; Li, Q.; Yu, Z.-X. *Org. Lett.* **2012**, *14*, 692.

(11) (a) Yu, Z.-X.; Wender, P. A.; Houk, K. N. *J. Am. Chem. Soc.* **2004**, *126*, 9154. (b) Yu, Z.-X.; Cheong, P. H.-Y.; Liu, P.; Legault, C. Y.; Wender, P. A.; Houk, K. N. *J. Am. Chem. Soc.* **2008**, *130*, 2378. (c) Liu, P.; Cheong, P. H.-Y.; Yu, Z.-X.; Wender, P. A.; Houk, K. N. *Angew. Chem., Int. Ed.* **2008**, *47*, 3939. (d) Hong, X.; Liu, P.; Houk, K. N. *J. Am. Chem. Soc.* **2013**, *135*, 1456.

(12) (a) Liu, P.; Sirois, L. E.; Cheong, P. H.-Y.; Yu, Z.-X.; Hartung, I. V.; Rieck, H.; Wender, P. A.; Houk, K. N. *J. Am. Chem. Soc.* **2010**, *132*, 10127. (b) Xu, X. F.; Liu, P.; Lesser, A.; Sirois, L. E.; Wender, P. A.; Houk, K. N. *J. Am. Chem. Soc.* **2012**, *134*, 11012.

(13) (a) Trost, B. M.; Indolese, A. *J. Am. Chem. Soc.* **1993**, *115*, 4361. (b) Trost, B. M.; Indolese, A.; Müller, T. J. J.; Treptow, B. *J. Am. Chem. Soc.* **1995**, *117*, 615. (c) Trost, B. M.; Krause, L.; Portnoy, M. *J. Am. Chem. Soc.* **1997**, *119*, 11319. (d) Trost, B. M.; Portnoy, M.; Kurihara, H. *J. Am. Chem. Soc.* **1997**, *119*, 836. (e) Trost, B. M.; Probst, G. D.; Schoop, A. *J. Am. Chem. Soc.* **1998**, *120*, 9228. (f) Trost, B. M.; Toste, F. D. *Tetrahedron Lett.* **1999**, *40*, 7739. (g) Chen, H.; Li, S. *Organometallics* **2005**, *24*, 872.

(14) (a) Trost, B. M.; Toste, F. D.; Shen, H. C. *J. Am. Chem. Soc.* **2000**, *122*, 2379. (b) Trost, B. M.; Shen, H. C. *Org. Lett.* **2000**, *2*, 2523. (c) Trost, B. M.; Shen, H. C. *Angew. Chem., Int. Ed.* **2001**, *40*, 2313. (d) Trost, B. M.; Shen, H. C.; Horne, D. B.; Toste, E. D.; Steinmetz, B. G.; Koradin, C. *Chem.—Eur. J.* **2005**, *11*, 2577.

(15) Trost, B. M.; Pinkerton, A. B.; Toste, F. D.; Sperrle, M. *J. Am. Chem. Soc.* **2001**, *123*, 12504.

(16) Trost, B. M.; Toste, F. D. *Angew. Chem., Int. Ed.* **2001**, *40*, 1114.

(17) Frisch, M. J.; et al. *Gaussian 09*, Rev. B.01; Gaussian, Inc.: Wallingford, CT, 2010.

(18) Zhao, Y.; Truhlar, D. G. *Theor. Chem. Acc.* **2008**, *120*, 215.

(19) Legault, C. Y. *CYLView*, 1.0b; Université de Sherbrooke: Canada, 2009; <http://www.cylview.org>.

(20) This possibility is being explored computationally, and suggests that the preferred pathway might be controlled by use of ligands to control the oxidation potential of the metal.

(21) Free energy surface scan from **5A** to **7A** indicates the dissociation of acetonitrile ligand with the C–C bond formation.

(22) Detailed comparisons of acetone and acetonitrile coordination are provided in the SI.

(23) The direct isomerization between **22** and **22-C2** is possible but requires a higher barrier (22.6 kcal/mol).